WTp53 induction does not override MTp53 chemoresistance and radioresistance due to gain-of-function in lung cancer cells

Andrew R. Cuddihy,[1] Farid Jalali,[1] Carla Coackley,[2] and Robert G. Bristow[1,2,3,4]

[1]Division of Applied Molecular Oncology; [2]Radiation Medicine Program, Ontario Cancer Institute, Princess Margaret Hospital (University Health Network); and Departments of [3]Radiation Oncology and [4]Medical Biophysics, University of Toronto, Toronto, Canada

Abstract

New molecular cancer treatment strategies aim to reconstitute wild-type p53 (WTp53) function in mutant p53 (MTp53)–expressing tumors as a means of resensitizing cells to chemotherapy or radiotherapy. The success of this approach may depend on whether MTp53 proteins are acting in a dominant-negative or independent gain-of-function mode. Herein, we describe an isogenic, temperature-sensitive p53 model ($p53^{A138V}$) in p53-null human H1299 lung cancer cells in which WTp53 can be selectively coexpressed with a temperature-sensitive MTp53 allele (A138V) during initial DNA damage and subsequent DNA repair. Cells expressing MTp53 alone or coexpressing induced WTp53 and MTp53 were tested for p53 transcription, G_1 and G_2 cell cycle checkpoints, apoptosis, and long-term clonogenic survival following DNA damage. Transient transfection of WTp53 into H1299 cells, or shift-down of H1299-$p53^{A138V}$ stable transfectants to 32°C to induce WTp53, led to increased $p21^{WAF1}$ expression and G_1 and G_2 arrests following DNA damage but did not increase BAX expression or apoptosis. In contrast, both transient and stable expression of the $p53^{A138V}$ mutant in p53-null H1299 cells (e.g. testing gain-of-function) at 37°C blocked $p21^{WAF1}$ induction following DNA damage. Cell death was secondary to mitotic catastrophe and/or tumor cell senescence. Overexpression of WTp53 did not resensitize resistant MTp53-expressing cells to ionizing radiation, cisplatinum, or mitomycin C. Our results suggest that human MTp53 proteins can lead to resistant phenotypes independent of WTp53-mediated transcription and checkpoint control. This should be considered when using p53 as a prognostic factor and therapeutic target. [Mol Cancer Ther 2008;7(4):980–92]

Received 7/12/07; revised 12/20/07; accepted 2/22/08.

Grant support: National Cancer Institute of Canada Operating Grant and Canadian Cancer Society Research Scientist Award (R.G. Bristow).

The costs of publication of this article were defrayed in part by the payment of page charges. This article must therefore be hereby marked *advertisement* in accordance with 18 U.S.C. Section 1734 solely to indicate this fact.

Note: Present address for A.R. Cuddihy: Division of Research Immunology/BMT and GISCT Program, Children's Hospital of Los Angeles, 4650 Sunset Boulevard, Los Angeles, CA 90027.

Requests for reprints: Robert G. Bristow, Radiation Medicine Program, Princess Margaret Hospital (University Health Network), University of Toronto, 610 University Avenue, Toronto, Ontario, Canada M5G 2M9. Phone: 416-946-3936; Fax: 416-946-4586. E-mail: rob.bristow@rmp.uhn.on.ca

doi:10.1158/1535-7163.MCT-07-0471

Introduction

Cells are subject to a variety of endogenous and exogenous genotoxic insult that can result in genetic instability and carcinogenesis. One of the key proteins that acts to preserve genetic stability following DNA damage is the p53 tumor suppressor protein, which enacts cell cycle arrest, facilitates DNA repair (1), or, in cases where the damage is severe, activates cell death (e.g. apoptosis, mitotic catastrophe, or terminal growth arrest depending on cell type). The importance of p53 in preventing carcinogenesis is perhaps best illustrated by the fact that over half of all human cancers have inactivating mutations of the p53 gene (2–6).

In the absence of DNA damage, wild-type p53 (WTp53) is maintained at low levels owing to rapid turnover of the protein through the ubiquitin-proteasome pathway via the MDM2 E3 ligase, which also serves to negatively regulate p53 function (7–10). In response to DNA damage, the ATM-CHK2, ATR-CHK1, and HIPK2 signaling pathways lead to a series of post-translational modifications including phosphorylation of WTp53 on discrete NH_2-terminal sites, including Ser^{15}, Ser^{20}, and Ser^{46}, thereby allowing WTp53 to become stabilized and activated (11–13). As such, the best understood function of activated WTp53 is that of a transcriptional factor, and several targets of p53 have been identified. Some, such as $p21^{WAF1}$ (14, 15) and 14-3-3σ (16) and the more recently identified *Ptprv* gene (17), have been shown to cause cell cycle arrest. Other WTp53 targets, such as Bax (18), PUMA (19), NOXA (20), and PIGs (21), induce apoptosis (22), although a role of transcription-independent p53-mediated apoptosis has been reported (23). Mutations [mutant p53 (MTp53)] in the core DNA-specific binding domain lead to abrogated p53-transactivation (4). Cell cycle arrest and the type of cell death are highly cell type and DNA damage specific, suggesting a bias of WTp53 toward specific targets. This hints at another layer of complexity with regards to the ability of p53 to determine the fate of a cell in response to DNA damage and thus regulate genetic instability.

Although cell cycle arrest is an indirect way for p53 to regulate the duration of DNA damage repair, there is increasing evidence emerging for a more direct role of WTp53 in the repair of DNA double-strand and single-strand breaks, mismatches, and DNA base damage (3). For

example, WTp53 can coimmunoprecipitate or colocalize with several DNA repair proteins (3) and WTp53 has been implicated in several specific DNA repair pathways, including homologous recombination, nonhomologous end joining, base excision repair, mismatch repair, and nucleotide excision repair in a transcription-independent manner (24–27). More recently, our laboratory showed that, following the onset of DNA damage, a subpool of total latent WTp53 was rapidly (that is, within 10 min) phosphorylated on Ser^{15} and formed discrete foci at the site of DNA double-strand breaks (DSB), colocalizing with activated H2AX (γ-H2AX), 53BP1, and the MRN complex (28) well in advance of any p53-mediated transactivation function. This chromatin localization of Ser^{15}-phosphorylated p53 represents a potentially novel function for p53 as a sensor of DNA damage to enact cycle checkpoints. MTp53 proteins may also act differently in DNA damage sensing within chromatin. Selected MTp53 proteins can interfere with MRE11 binding to breaks leading to abrogation of the ATM signaling cascade following DNA damage (29).

MTp53 proteins may drive a mutator phenotype resulting in chemoresistance and radioresistance through differential p53 transactivation, abrogated cell cycle arrests, and altered DNA damage sensing and repair (3, 30). For example, in most non-small cell lung cancers, p53 can be disrupted through mutation or decreased expression leading to a poor prognosis (31). As a result, the balance of expression of p53 target genes, such as $p21^{WAF1}$, *Bax*, and *PUMA*, may alter the biological behavior and sensitivity of tumor cells to cancer therapy (32). However, the cellular context and DNA damage pathway may be very important in determining the fate of p53-deficient cells as they may acquire resistance to ionizing radiation (IR).

Several novel p53-based molecular targeting agents have been recently described, which act to augment WTp53 expression or revert MTp53 proteins to a WTp53 conformation. These therapies have been suggested as novel monotherapies or as relative sensitizers when used in combination with chemotherapy and radiotherapy in several cancers (31, 33, 34). Whether this maneuver is successful may depend on whether WTp53 function can override independent MTp53 effects [e.g., gain-of-function (GOF)] with respect to the cellular sensitivity to DNA-damaging agents (35).

Few studies have investigated both MTp53 GOF and dominant-negative models as a determinant of cell survival following radiotherapy or chemotherapy within the same model. Many laboratories, including our own, have shown increased resistance and tumor growth in p53-null cells expressing MTp53 alleles (36–39). However, these studies required testing of multiple individual null or MTp53 clones susceptible to irreversible genetic changes and clonal selection that could bias resulting phenotypes. As permanent overexpression of WTp53 is toxic to p53-null cells (40–44), an isogenic system that allowed reversible, short-term induction of WTp53 during exogenous DNA damage and repair would be useful to understand the potential therapeutic effect of WTp53 when expressed in MTp53-expressing cells.

Herein, we describe a novel, isogenic temperature-sensitive p53 model in H1299 lung cancer cells in which MTp53 is expressed alone or simultaneously with an induced WTp53 protein during initial DNA damage and the process of DNA repair. The model uses a temperature-sensitive mutant of human p53, containing an alanine-to-valine mutation at codon 138 ($p53^{A138V}$). We show that transactivation of WTp53 gene expression and WTp53 function at the time of DNA damage does not resensitize MTp53-expressing cells, which have acquired resistance to DNA-damaging agents, consistent with a GOF phenotype for this human p53 mutant. We discuss our data in the context of the use of p53 for prognostication and the prediction of response to novel p53-directed therapies.

Materials and Methods

Vector Construction and Transfections into H1299 Cells

WTp53 was subcloned in frame with COOH terminus of the HcRed-C1 vector (Clontech) by digesting YFP-WTp53 (28) using *Hin*dIII and *Bam*HI sites and ligating into the respective sites of the HcRed vector to generate HcRed-$p53^{WT}$. The $Ala^{138}Val$ temperature-sensitive mutation was introduced into HcRed-$p53^{WT}$ using the QuikChange site-directed mutagenesis kit (Stratagene) and the primers AAGATGTTTTGCCAACTGGTCAAGACCTGCCCTGTGCAG (forward) and CTGCACAGGGCAGGTCTTGACCAGTTGGCAAAAGATCTT (reverse) to generate HcRed-$p53^{A138V}$. The mutation was confirmed by sequencing both strands. All cDNAs used were purified using the Maxiprep DNA purification kit (Qiagen).

The p53-null H1299 human lung carcinoma cell line was kindly provided by Dr. Simon Powell (Washington University). Cells were maintained in RPMI 1640 supplemented with antibiotics, 20 mmol/L HEPES (pH 7.5), and 10% FCS. Cells were routinely maintained in a humidified 37°C incubator in the presence of 5% CO_2. Cells were transfected with 5 μg HcRed vector, HcRed-$p53^{A138V}$, or HcRed-$p53^{WT}$ using Metafectene (Biontex) according to the manufacturer's instructions. For transient transfections, cells were studied at 24 h post-transfection. To generate stable populations, cells were selected using G418 (Calbiochem) at 24 h post-transfection. At the same time, individual G418-resistant clones were isolated using the single-cell limiting dilution method. The remaining cells were pooled to give a heterogenous population of G418-resistant cells. All G418-resistant cells were routinely maintained in RPMI 1640 as above plus 250 μg/mL G418 at the permissive temperature of 37°C (p53 in MTp53 conformation).

Flow Cytometry and Cell Proliferation Assays

Cellular proliferation at 37°C or 32°C was assessed by initially plating 1×10^4 cells into 6-cm dishes and counting cells daily as a function of time over a 7-day period. The following treatments were studied for their effect on cell

proliferation: (*a*) maintaining 37°C for the entire duration, (*b*) a short-term shift to 32°C for either 9 or 24 h and then shifting back to 37°C, and (*c*) maintaining cells at 32°C for the 7-day duration. For each count, cells were trypsinized, washed, stained with trypan blue, and counted on a hemocytometer to quantitate the number of viable cells over time.

To assay DNA content in diploid H1299 cells, cells were resuspended in ice-cold 70% ethanol and fixed at -20°C overnight. Cells were then washed extensively with ice-cold PBS and resuspended in PBS plus 50 μg propidium iodide (Sigma) and 25 μg RNase A. DNA content was analyzed on a FACScan or FACSCalibur using CellQuest software (Becton Dickinson) as described previously (45).

Protein Extraction, Immunoprecipitation, and Immunoblotting

Cells were collected and washed with ice-cold PBS. Whole-cell extracts were obtained by resuspending the cells in 10 pellet volumes of extraction buffer [50 mmol/L Tris-HCl (pH 8.0), 0.5 mmol/L EDTA, 125 mmol/L NaCl, 0.5% NP40] supplemented with protease and phosphatase inhibitors. Following 15 min on ice, lysates were clarified by centrifuging at 14,000 rpm for 10 min, and the supernatant was collected for analysis. Cytoplasmic and nuclear extracts were obtained using the Dignam method (46). Briefly, collected cells were gently resuspended in cytoplasmic lysis buffer [25 mmol/L KCL, 5 mmol/L $MgCl_2$, 50 mmol/L Tris-HCl (pH 8.0) 0.5% NP40 supplemented with protease and phosphatase inhibitors]. Following 10-min incubation on ice, the nuclei were pelleted by centrifuging for 5 min at 3,000 rpm. The supernatant-containing cytoplasmic proteins were transferred to a fresh 1.5 mL Eppendorf tube. Following a gentle washing in cytoplasmic lysis buffer, the nuclei were lysed in nuclear lysis buffer [0.5 mol/L NaCl, 1.5 mmol/L $MgCl_2$, 10 mmol/L Tris-HCl (pH 8.0), 5 mmol/L EDTA, 0.1% NP40 supplemented with protease and phosphatase inhibitors]. After 30 min on ice with occasional vortexing, the suspension was clarified by centrifuging at 13,000 rpm for 10 min. All protein quantitations were carried out using the BCA Assay reagent kit (Pierce) and analyzed at 545 nm on a plate reader (Bio-Rad).

For immunoprecipitations, protein lysate (250-500 μg) was incubated with the mouse monoclonal anti-p53 antibodies PAb240 (mutant specific), PAb1620 (wild-type specific; Calbiochem), or Bp53-12 (pan-specific; Santa Cruz). Nonreactive mouse IgG was used as a negative control. Protein G-Sepharose beads (50 μL; 50% slurry; Amersham) was added and the immune complexes were pulled down over 1 h at 4°C under rotation. Beads were washed extensively with lysis buffer to remove any nonbound proteins and lysed by boiling in the presence of Laemmli buffer.

For Western blotting, released immune complexes or 25 to 50 μg protein lysates boiled in Laemmli buffer were resolved on either 8% or 15% SDS-PAGE gels. Proteins were transferred onto nitrocellulose membranes (Schleicher and Schuell). Membranes were probed with the anti-p53 Bp53-12 antibody, mouse monoclonal anti-$p21^{WAF1}$ antibody (Calbiochem), rabbit polyclonal anti-actin antibody (Sigma), rabbit polyclonal anti-phospho-Ser^{15} p53 antibody (CST), rabbit polyclonal anti-Ser^{10}-P histone H3 antibody (Upstate), or rabbit polyclonal anti-HcRed antibody (Clontech). Proteins were visualized first by probing with horseradish peroxidase–conjugated anti-mouse or anti-rabbit IgG (Amersham) and then by chemiluminescence using the Western Lightening kit (Perkin-Elmer) and exposing to X-ray film (Kodak). Where indicated, densitometric measurements of proteins were done using ImageJ software (NIH). Target proteins were first normalized to actin protein levels and fold induction was calculated based on deviations from the $t = 0$ controls.

RNA Isolation, Reverse Transcription, and Quantitative Real-time PCR

Total cellular RNA was isolated from cells using the RNeasy kit (Qiagen). RNA was quantitated on a Nanodrop ND-100 spectrophotometer (peqlab Biotechnology). One microgram of the sample RNA or human reference RNA (Stratagene) was treated with DNase I (Roche) according to the manufacturer's instruction. Samples were reverse transcribed using random hexamer primers and the TaqMan Reverse Transcription Kit (ABI).

Real-time PCR primers and fluorescent probes of target genes and endogenous controls were obtained as Assays-On-Demand (ABI). Each gene-specific PCR reaction was a master mix consisting of human reference or sample cDNA, 1× Assays-on-Demand, and 1× TaqMan Universal PCR Master Mix (ABI) and aliquoted in triplicate onto a 384-well plate so that each reaction contained 15 ng sample cDNA or 30, 15 and 7.5 ng human reference cDNA. Reactions were done in an ABI 7900 thermal cycler (Applied Biosystems) with SDS software (ABI). The fluorescence intensity threshold was set at 0.2, representing a point where the intensity rises above the baseline into a logarithmic curve for all samples. The reaction cycle threshold (Ct) representing the cycle number that intersected along the curve at the designated fluorescence intensity threshold was obtained. Because each sample/gene assay combination was done in triplicate, the average Ct value and SD was obtained.

Analysis was done using the relative standard curve quantification method (47). Briefly, standard curves for each gene were established from the average Ct values obtained from the human reference cDNA. The slope of the resulting curve is a measure of the PCR efficiency. Average Ct values of the experimental samples were then corrected for differences in PCR efficiency among the various genes. These corrected values were then normalized to the experimental control sample for each gene and then normalized to the values for the housekeeping gene (18S) for each sample.

Immunofluorescent Microscopy and Apoptosis/Senescence-Associated β-Galactosidase Assays

Cells were fixed and permeabilized as described previously (28). Cells were stained with mouse monoclonal γ-H2AX antibody (Upstate) at 1:500 dilution or mouse monoclonal activated caspase-3 antibody (Cell Signaling) at

1:200 dilution and counterstained with Alexa 488–conjugated anti-mouse secondary at a 1:500 dilution (Molecular Bioprobes). DNA staining was accomplished with 4′,6-diamidino-2-phenylindole before microscopy.

Exogenous protein localization and apoptosis were examined by simultaneously fixing and staining in 1 mL PBS containing 10% formalin and 10 μmol/L Hoechst 33342 (Sigma) for 30 min at room temperature. Following fixation,

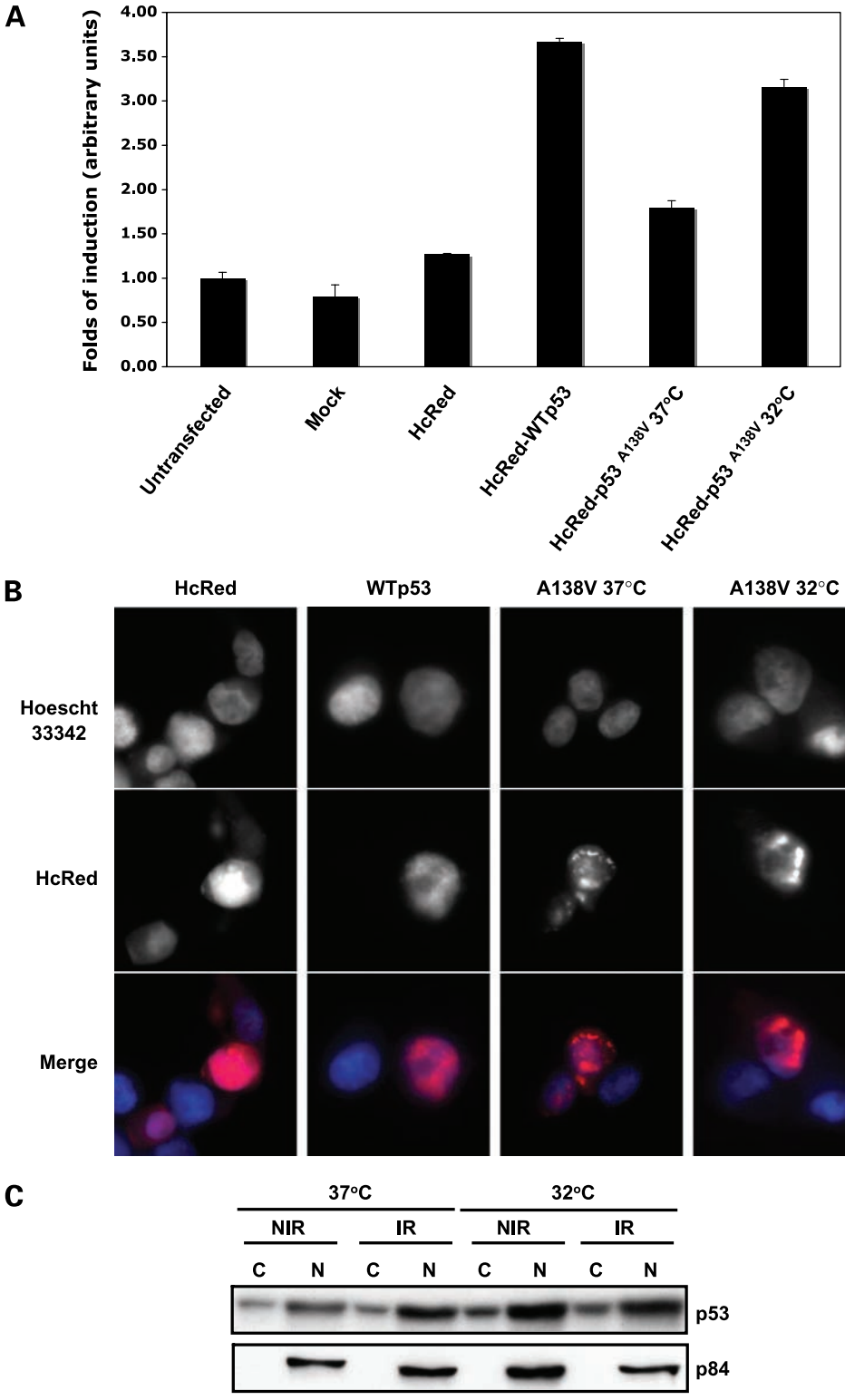

Figure 1. Transient transfection of p53 induces $p21^{WAF}$ following nuclear accumulation. **A,** H1299 cells were mock transfected, transfected with HcRed alone, or transfected with HcRed-WTp53 and HcRed-$p53^{A138V}$ (under conditions of 37°C or a shift to 32°C post-transfection). Twenty-four hours post-transfection, cells were harvested and assessed for levels of $p21^{WAF1}$ mRNA. Bar plot shows qRT-PCR results for induction of $p21^{WAF1}$ mRNA. *Bars,* SD of triplicate reactions. **B,** cellular localization of HcRed fusion proteins. Transiently transfected cells were fixed in formalin and stained with Hoechst 33342 and examined for DNA staining (*top*) and HcRed (*middle*). *Bottom,* a merge of *top* and *middle*. Note intranuclear staining pattern of MTp53 near nuclear matrix at either 37°C or 32°C, which colocalizes with DNA. **C,** biochemical localization of HcRed-$p53^{A138V}$. Cytoplasmic (*C*) and nuclear (*N*) fractions were isolated from cells kept at 37°C or 32°C in the absence of DNA damage (NIR) or 2 h following 10 Gy (IR). Lysates were resolved on SDS-PAGE and blotted for p53. As a control for fractionation of extracts, the nuclear lamin protein p84 was used (*bottom*).

cells were centrifuged briefly, most of the supernatant was discarded, and the cell pellet was resuspended. Cell suspension (20 μL) was spotted onto a glass slide and overlaid with a coverslip for microscopy.

Senescence-associated β-galactosidase (SA-β-galactosidase) was detected using a SA-β-galactosidase assay kit according to the manufacturer's instructions (Cell Signaling).

Cells were examined using either an Axiovert wide-field microscope under control of Northern Eclipse software (28).

Induction of DNA Damage and Clonogenic Assays

DNA DSBs were induced by cellular γ-irradiation using a Gammacell irradiator (Noridon International) with a Cs^{137} source as described previously (48). Cells were prepared for UV irradiation by removing all media and a PBS wash from tissue culture plates and then irradiated with 10 J/m^2 using a 254 nm Stratalinker UV source (Stratagene). For drug treatments, cells were exposed 250 μmol/L mitomycin C (MMC) for 1 h or 1 μg/μL cisplatinum (cDDP) for 1 h.

For clonogenic assays, H1299-dR-GFP cells stably expressing HcRed or HcRed $p53^{A138V}$ were plated into six-well dishes at an appropriate density according to the treatment given. After ~4 to 6 h, some of the cells were shifted to 32°C and incubated for a further 9 h to allow for the tsp53 to acquire a wild-type conformation and for the cells to stabilize. Before doubling, the cells were then irradiated or treated with drug as indicated. The cells were then returned to 37°C or 32°C as appropriate. Four or 24 h after initial induction of DNA damage, some of the cells were shifted from 32°C to 37°C and left for 7 to 10 days to allow for colony formation. Colonies were fixed and stained using methylene blue in 70% ethanol and scored to calculate the relative surviving fraction as described previously (37).

Results

Expression of WTp53 or $p53^{A138V}$ at 32°C Both Lead to Nuclear Accumulation and $p21^{WAF}$ Induction in H1299 Cells

The WTp53 gene was cloned into a HcRed vector to express fluorescent HcRed-p53 fusion proteins. In addition to HcRed-$p53^{WT}$, a temperature-sensitive variant of p53 containing an alanine-to-valine mutation at codon 138 (HcRed-$p53^{A138V}$) was also generated. This p53 variant is maintained in a mutant conformation at 37°C but can acquire a wild-type conformation at 32°C (49).

As reported previously, attempts to generate H1299 cells that stably expressed HcRed-$p53^{WT}$ were not successful likely due to the toxic effects of WTp53 overexpression in a p53-null background (40–44). However, H1299 cells transfected with HcRed-$p53^{A138V}$ and maintained at the permissive temperature of 37°C gave rise to G418-resistant colonies and both single-cell clones and pooled populations stably expressing HcRed-p53. We therefore used a mixture of both transient and stable transfectants to determine WTp53 and MTp53 function in H1299 cells.

Using transient transfections, we initially investigated the subcellular location and function of exogenous WTp53 and MTp53 in p53-null H1299 cells. The empty HcRed vector, HcRed-$p53^{WT}$, or HcRed-$p53^{A138V}$ were transiently transfected into H1299 cells. Expression of HcRed-$p53^{A138V}$ at the restrictive temperature and HcRed-$p53^{WT}$ caused an induction of the $p21^{WAF1}$ gene based on quantitative real-time PCR (qRT-PCR; Fig. 1A). Expression of $p53^{A138V}$ at 37°C induced a reduced amount of $p21^{WAF1}$ at the RNA level.

Using immunofluorescent microscopy following transient transfection, we observed that HcRed-$p53^{WT}$ was pan-nuclear, whereas HcRed-$p53^{A138V}$ formed aggregates within the inner nuclear membrane consistent with previous reports of MTp53 proteins binding to the nuclear matrix (50). HcRed alone was almost always cytoplasmic at either temperature. Given the results of the transient transfections, we used biochemical cell fractionation techniques to obtain cytoplasmic and nuclear protein extracts to determine the cytoplasmic-to-nuclear ratio of HcRed-$p53^{A138V}$ at both 37°C and 32°C after irradiation in stable transfectants. Consistent with the microscopy experiments, we observed HcRed-$p53^{A138V}$ to be predominantly nuclear at both permissive and restrictive temperatures (see Fig. 1C). This is in contrast to previous reports using the murine orthologue of this mutant that suggested a cytoplasmic localization at 37°C and nuclear localization at 32°C (44, 51).

Of note, transfection of HcRed-$p53^{WT}$ or HcRed-$p53^{A138V}$ at either 32°C or 37°C did not induce the *Bax* gene nor lead to increased apoptosis based on morphologic staining with 4′,6-diamidino-2-phenylindole or Hoechst 33342 over multiple experiments (data not shown).

We conclude that HcRed-$p53^{WT}$ and HcRed-$p53^{A138V}$ expressed at 32°C are nuclear-acting and functional for p53-dependent gene expression of $p21^{WAF1}$ in p53-null H1299 cells. We therefore conducted all further studies with stable HcRed-$p53^{A138V}$-expressing transfectants.

Short-term Induction of Functional WTp53 Is Nontoxic in H1299-$p53^{A138V}$ Transfectants

Although described as temperature sensitive, the $p53^{A138V}$ protein may not be temperature specific in terms of either 100% MTp53 or WTp53 conformation at permissive and restrictive temperatures. In the absence of DNA damage, WTp53 is very unstable and is rapidly turned over via the ubiquitin-proteasome pathway, whereas increased stability is one of the hallmarks of MTp53. A similar result has been observed with the murine $p53^{A135V}$ mutant (41, 51).

To fully characterize the HcRed-$p53^{A138V}$ H1299 model system in the absence of DNA damage, we determined the relative levels of WTp53 versus MTp53 protein using the p53 conformation-specific antibodies PAb1620 to detect WTp53 (52) and PAb240 to detect MTp53 (53) at 37°C (t = 0) and at various periods after a shift to 32°C where some p53 acquires a wild-type conformation (Fig. 2A, *i*). WTp53 first appears within 3 h at 32°C and was stable at periods of up to 24 h. However, even at 32°C, MTp53 is

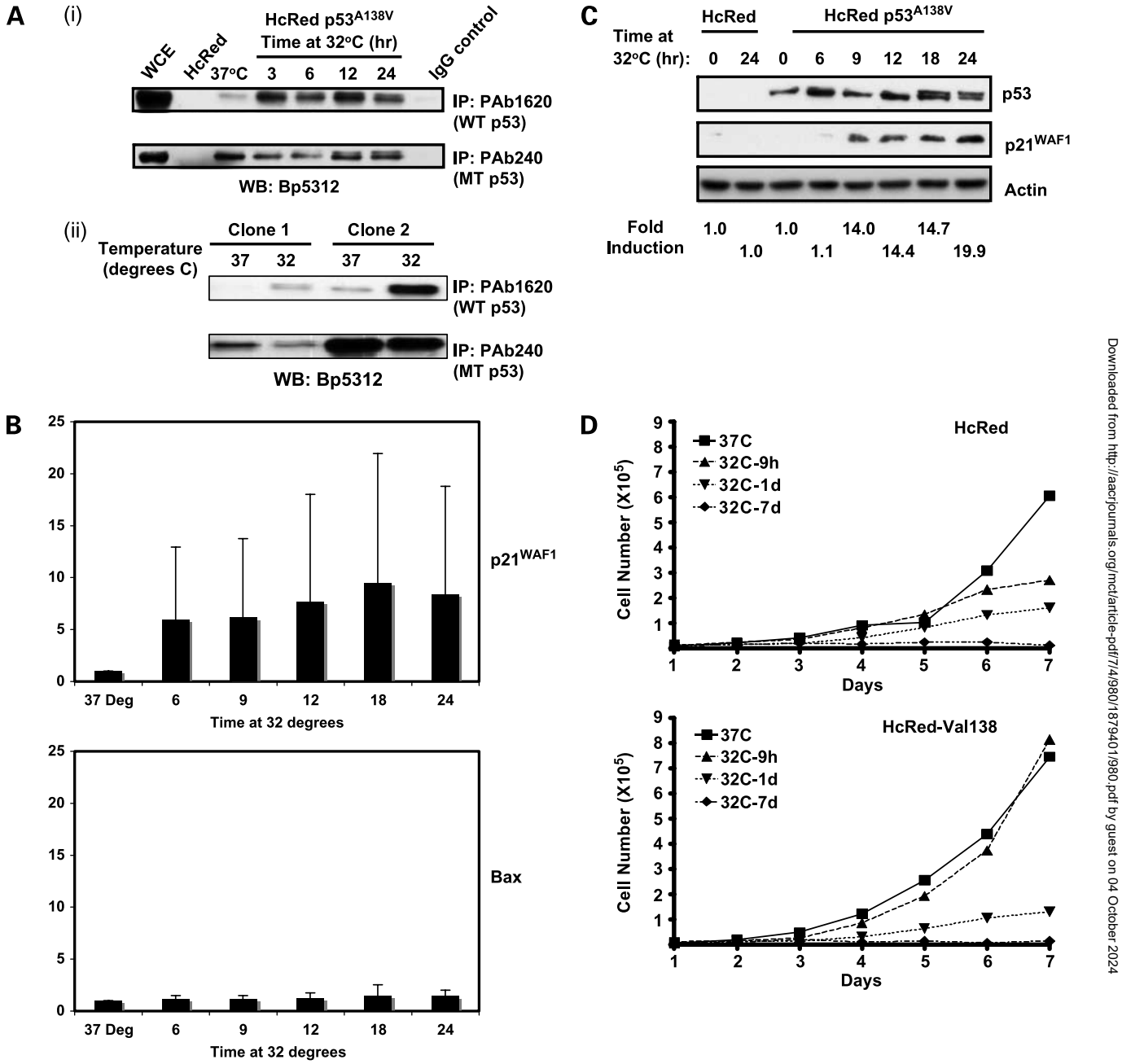

Figure 2. Expression of MTp53 and coexpression of MTp53 and WTp53 stable expression following temperature shift. **A,** WTp53 versus MTp53 antibody reactivity in stable HcRed-p53^{A138V} transfectants. Stable pools (i) or two selected clones (ii) of HcRed-p53^{A138V}-expressing cells were shifted to 32°C and harvested at various time points along with cells kept at 37°C, representing $t = 0$ h. In the case of the two clones, only cells harvested at 37°C or kept at 32°C for 24 h were used. Equal amounts of the same lysates from each time point were immunoprecipitated with either wild-type-specific antibody (PAb1620) or mutant-specific antibody (PAb240). Immunoprecipitates were resolved on SDS-PAGE and probed with a pan-specific p53 antibody (Bp53-12). As negative controls for this experiment, cells expressing HcRed were immunoprecipitated with either PAb1620 or PAb240 and cells expressing HcRed^{A138V} were immunoprecipitated with nonreactive mouse IgG. **B,** p53-dependent gene expression in stable HcRed-p53^{A138V} transfectants. Total mRNA from **A** was isolated and reverse transcribed and the resulting cDNA was subjected to qRT-PCR with gene assays specific for *p21^{WAF1}* (*top*) or *Bax* (*bottom*) genes and normalized to mRNA levels of the 18S housekeeping gene. *Bars,* SE from three independent experiments. **C,** induction of p53 and p21^{WAF1} in HcRed-p53^{A138V} stable transfectants with temperature shift to 32°C. Cells were harvested at various times over 24 h following temperature shift-down and blotted for p53 and p21^{WAF1} proteins. Control HcRed cells were harvested at 0 h (at 37°C) and 24 h post-shift to 32°C. Shown also is a loading control for actin protein. *Numbers at the bottom,* fold increase of p21^{WAF1} protein relative to actin levels over the time course using quantitative densitometry. **D,** cell proliferation in HcRed-p53^{A138V} cells is temperature dependent. Cells expressing HcRed (*top*) or HcRed-p53^{A138V} (*bottom*) were plated at the same density and harvested every 24 h up to 7 days. The plots show cells kept at 37°C (*squares*) throughout, cells kept at 32°C for 9 h then shifted to 37°C (*upright triangles*), cells kept at 32°C for 24 h then shifted to 37°C (*downward triangles*), and cells kept at 32°C for the duration of the experiment (*diamonds*).

always detectable at periods up to 24 h. To eliminate the possibility that these results were due to the use of a heterogenous population of G418-resistant clones, two clones generated from single cells were also examined. Similar to what was seen with the populations, the amount of WTp53 increases significantly after shift-down, whereas the MTp53 is still present in significant amounts at 24 h following a shift to 32°C (Fig. 2A, *ii*).

The consequences of coexpression of WTp53 and MTp53 was determined first by performing qRT-PCR from H1299-p53^{A138V} cells maintained at 37°C (t = 0) where p53 is inactive or shifted to 32°C in the absence of DNA damage. Figure 2B shows the induction of $p21^{WAF1}$ and *Bax* mRNA levels (each data normalized to 18S rRNA) relative to the basal levels of $p21^{WAF1}$ and Bax mRNA expressed in the t = 0 control. The data are consistent with a favored induction of $p21^{WAF1}$ over *Bax* similar to the transient transfections. The large error bars for $p21^{WAF1}$ reflect a tremendous variation in the amount of fold induction observed from one experiment to the next, but we consistently observed an induction of $p21^{WAF1}$ in the three independent experiments and no induction of *Bax* as reflected by the small error bars.

It is worth noting that at no time during shift-down did we detect apoptosis using fluorescence-activated cell sorting analysis (sub-G_1 peak), morphologic analyses, or activated caspase-3 assays (data not shown), suggesting that the apoptotic response is not operational in this model. This is in line with previous reports using the murine orthologue in which cells expressing p53^{A135V} were

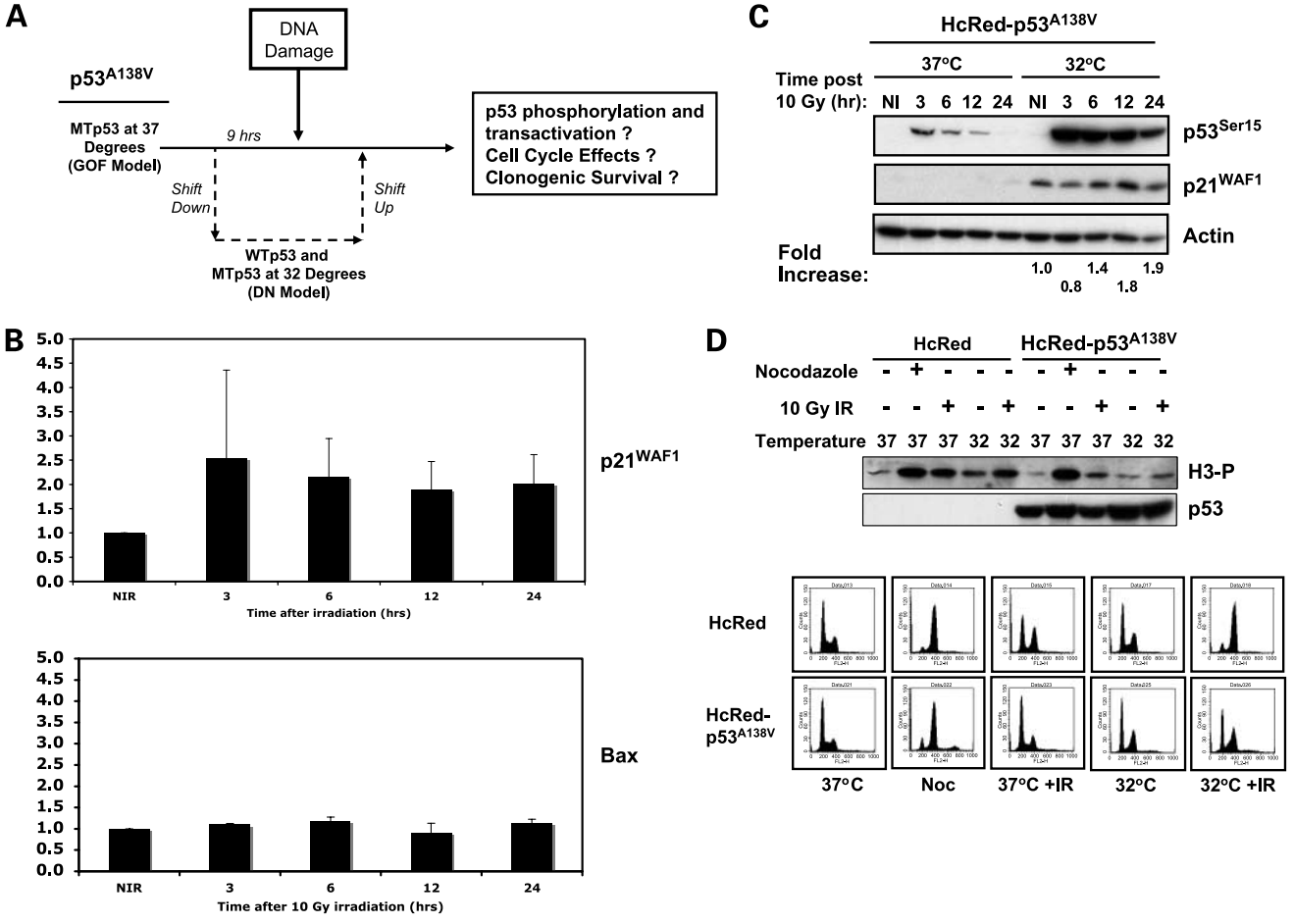

Figure 3. Response to DNA damage by H1299 cells expressing HcRed-p53^{A138V}. **A,** schematic diagram showing use of temperature-sensitive cells to test DNA damage responses in the context of MTp53 GOF and MTp53/WTp53 dominant-negative models. **B,** qRT-PCR of $p21^{WAF1}$ (*top*) and *Bax* (*bottom*) (*bottom*) gene mRNA. Cells were kept at 37°C or shifted to 32°C for 9 h before exposure to 10 Gy IR. mRNA levels were normalized to the nonirradiated sample. *Bars,* SE of three independent experiments. Note again the augmentation of $p21^{WAF1}$ mRNA in response to DNA damage in contrast to *Bax* mRNA. **C,** Western blotting for p53 protein phosphorylation at Ser^{15} and downstream p21^{WAF1} protein. Cells were kept at 37°C or shifted to 32°C for 9 h before exposure to 10 Gy IR and harvested at the indicated times following IR. Cell lysates were probed for phosphorylated Ser^{15}-p53, p21^{WAF1}, or actin (loading control). Densitometry confirmed 2-fold increase in p21^{WAF1} protein above the nonirradiated sample at 12 and 24 h. **D,** effect of IR on cell cycle distribution and histone H3 phosphorylation. Cells were maintained at 37°C (*bottom,* 37°C) or shifted to 32°C for 9 h (*bottom,* 32°C) before exposure to 10 Gy DNA damage (*bottom,* 37°C + IR or 32°C + IR). Twenty-four hours following DNA damage, cells were harvested and fixed for fluorescence-activated cell sorting analysis. As a control, both cell lines were treated with nocodazole (*Noc*) at 37°C for 18 h (*bottom*). Lysates were also prepared from these cells and resolved on SDS-PAGE and probed for histone H3 phosphorylation (*H3-P*) or p53 protein expression.

underwent cell growth arrest but maintained 100% viability for up to 1 week at the lower temperature when p53 is in a wild-type conformation (44). Western blotting of the stable transfectants shifted to 32°C for various periods showed that $p21^{WAF1}$ protein was induced above basal levels of p21 expressed at 37°C ($t = 0$) where p53 is in an inactive conformation and was recognized with the pan-specific anti-p53 antibody Bp53-12 (Fig. 2C).

Finally, we examined the effect of the temperature shift-down on cell proliferation in our model system. When cells expressing either HcRed or HcRed-$p53^{A183V}$ were maintained at 37°C, cells proliferated exponentially. Shifting to 32°C for 9 h (a common incubation time used to achieve WTp53 conformation in some temperature-sensitive p53 studies; ref. 49) and returning the cells to 37°C for a further 7 days minimally affected proliferation in HcRed-$p53^{A183V}$ cells and moderately slowed proliferation in HcRed-only cells. However, when either cell transfectant category was maintained at 32°C for extended periods (that is, 24 h and then returned to 37°C or kept at 32°C over 7 days); proliferation was markedly decreased (Fig. 2D). This suggests that long-term incubation at 32°C is detrimental to the proliferation of both HcRed-$p53^{A138V}$ and HcRed-only cells. Our data support that a shift-down in temperature to 32°C for periods up to 9 h in this system minimally affects cellular proliferation in spite of the increase in WTp53 in the HcRed-$p53^{A138V}$. The 9-h incubation time can therefore used to determine the effects of WTp53 and MTp53 expression in combination with DNA damage without causing a pleiotropic effect.

G_1 and G_2 Checkpoint Responses to DNA Damage in H1299-$p53^{A138V}$ Cells Expressing MTp53 Alone or Coexpressing WTp53 and MTp53

After characterizing the temperature sensitivity of the model, we next used H1299-$p53^{A183V}$ cells to determine the ATM-p53-$p21^{WAF1}$ response to DNA damage when either MTp53 alone is expressed (GOF model) or when MTp53 and WTp53 are coexpressed (dominant-negative model). We therefore irradiated H1299-$p53^{A183V}$ cells at 37°C or following shift-down to 32°C for 9 h and tested for p53 activation, phosphorylation, and altered cell cycle distribution (see Fig. 3A).

qRT-PCR analyses in WTp53-expressing H1299 cells confirmed that the DNA breaks caused by IR further induces the *$p21^{WAF1}$* gene beyond that achieved by temperature shift alone. In contrast, the *BAX* gene was unresponsive to DNA damage (Fig. 3B). Similarly, $p21^{WAF1}$ protein expression appeared to be augmented nearly 2-fold in response to DNA damage when normalized to the $p21^{WAF1}$ protein levels attained due to temperature shift alone before DNA damage (Fig. 3C). $p21^{WAF1}$ expression was not observed in HcRed cells at either temperature even after IR and was also not observed in H1299-$p53^{A138V}$ cells maintained at 37°C following IR.

We also observed that Ser^{15} phosphorylation of p53 was greater following DNA damage in cells expressing WTp53 in comparison with cells expressing solely MTp53 (Fig. 3C) and supports a previous finding that NH_2-terminal phosphorylation of p53 by DNA damage is conformation dependent (54, 55).

It is worth noting that, in all our experiments, a slower-migrating form of p53 was consistently observed when the cells were shifted to 32°C (Fig. 2C). Treating the extracts with λ-phosphatase eliminated the upper band, suggesting that the shift to 32°C causes some latent conformation-dependent phosphorylation (data not shown). This phenomenon was further investigated using a limited panel of NH_2-terminal phosphospecific antibodies (Ser^6, Ser^9, Ser^{15}, Ser^{20}, Ser^{37}, and Ser^{46}) as well as Ser^{392}. No temperature-dependent changes in the phosphorylation levels at these particular sites were observed (data not shown), suggesting that the WTp53-specific phosphorylation site(s) are not detected with the panel of antibodies used in this study. These data suggest that the observed induction of $p21^{WAF1}$ and other p53-inducible genes could occur independently of DNA damage–induced NH_2-terminal phosphorylation (56) and that there are other crucial latent phosphorylation sites that are WTp53 specific.

To test the function of WTp53 expression in the H1299-$p53^{A138V}$ cells, we characterized cellular arrest at both G_1-S and G_2-M checkpoints in irradiated HcRed and HcRed-$p53^{A138V}$ cells at 37°C ad 32°C (Fig. 3D). Phosphorylation on Ser^{10} of histone H3 was examined as a marker for cells in mitosis and helps distinguish whether the cells in the G_2-M peak consist of a mixture of both G_2 and M cells [high H3 phosphorylation or solely consist of cells blocked in G_2 (low H3 phosphorylation; ref. 57)]. In the absence of DNA damage, the fluorescence-activated cell sorting profiles (*bottom*) of both cell lines show asynchronous growth with minimal H3 phosphorylation (*top*). As a control for H3 phosphorylation, both cell lines were treated with the microtubule inhibitor, nocodazole, which arrests cells in early mitosis. This resulted in an accumulation of cells with 4N DNA content and an increase in detectable H3 phosphorylation (Fig. 3D, *top*).

When the cells maintained at 37°C were irradiated, cells expressing HcRed showed an increased accumulation at the G_2-M phase. Irradiated cells expressing HcRed-$p53^{A138V}$ remained largely in G_1 with a much smaller G_2-M accumulation. Both cell lines showed increased H3 phosphorylation following DNA damage indicating cells in both G_2 and M phases. The presence of a strong G_1 peak in HcRed-$p53^{A138V}$ cells at the permissive temperature following irradiation is quite surprising. It could indicate that the small amount of WTp53 present even at the permissive temperature, which becomes phosphorylated in response to DNA damage (Fig. 3C), is potent enough to cause a G_1 arrest. It also indicates that MTp53 in this model does not have a dominant-negative effect on the WTp53 protein insofar as functional cell cycle control.

At 32°C, the DNA content of unirradiated HcRed cells did not change compared with cells at 37°C. There was a slight increase in cells in G_2 in the HcRed-$p53^{A138V}$ cells under the same conditions as evidenced by the lack of H3 phosphorylation. Following DNA damage at 32°C, the cells expressing HcRed accumulated in G_2-M peak accompanied

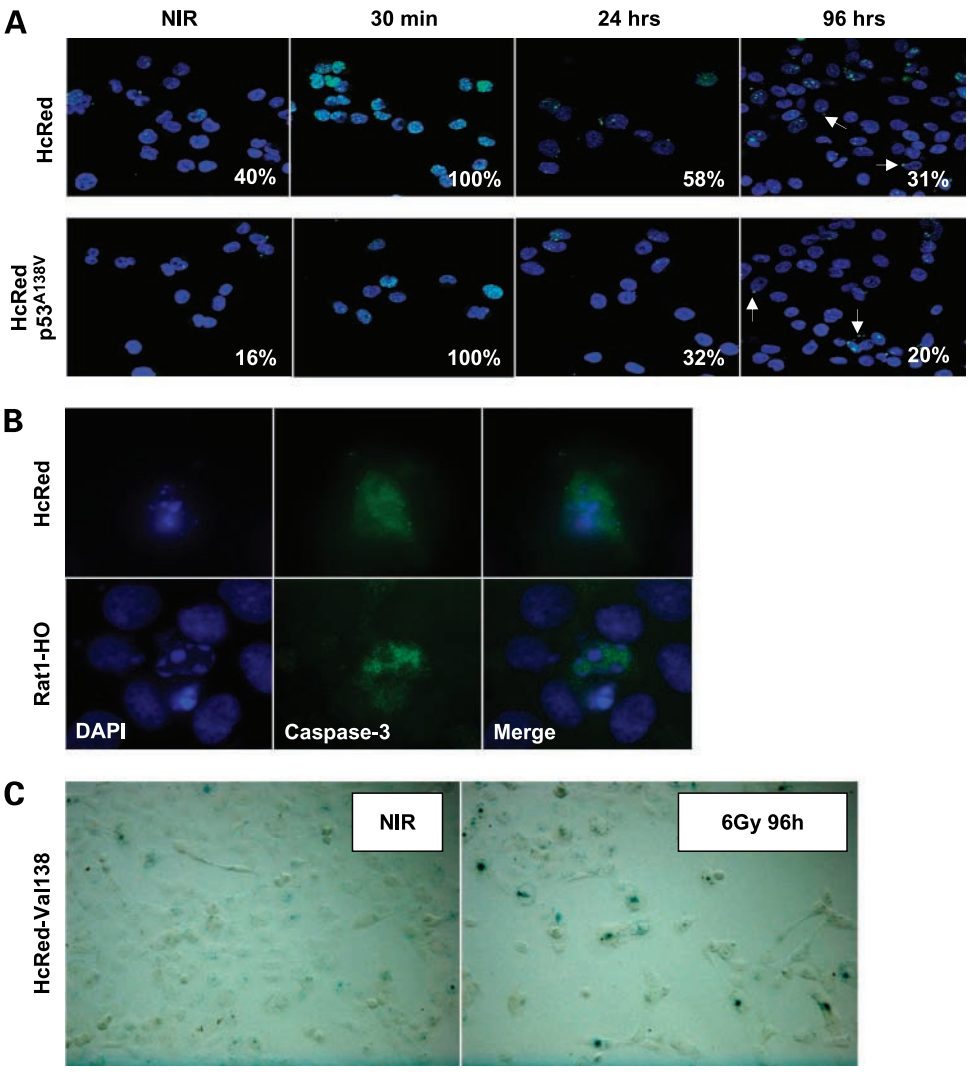

Figure 4. H1299-p53^{A138V} cell survival following exposure to DNA DSBs and intrastrand cross-links. **A,** representative experiment showing presence of γ-H2AX foci in HcRed and HcRed-p53^{A138V} cells. In this experiment, cells were maintained at 37°C throughout. Before irradiation (NIR) and at 30 min, 24 h, and 96 h following a dose of 2 Gy, cells were fixed and stained with mouse monoclonal γ-H2AX antibody and counterstained with 4′,6-diamidino-2-phenylindole to allow visualization of DNA. The percentages (*bottom right*) are the proportion of cells with >5 visible γ-H2AX foci. **B,** induction of apoptosis. HcRed cells or Rat1-HO cells exposed to 6 Gy IR and maintained at 37°C were fixed and stained for activated caspase-3 as a marker of apoptosis and counterstained with 4′,6-diamidino-2-phenylindole. Apoptosis was observed minimally in irradiated H1299 cell lines (see text for details). **C,** HcRed-p53^{A138V}-expressing cells stained with SA-β-galactosidase before (NIR; *left*) and 96 h following exposure to 6 Gy IR (*right*). Cells were examined under phase-contrast conditions allowing for visualization of blue β-galactosidase stain. Similar staining patterns were seen in HcRed cells.

by a significant amount of H3 phosphorylation. Given that the G_2-M checkpoint is generally intact even in cells lacking p53 (3), this is not surprising. However, WTp53-expressing HcRed-p53^{A138V} cells showed evidence of accumulation at both G_1 and G_2 peaks. The lack of H3 phosphorylation in these cells indicates that the cells were blocked from entering mitosis in a p53-dependent manner. The fluorescence-activated cell sorting profiles did not show at any time an increase in a population of cells with sub-G_1 DNA content, confirming a lack of apoptosis in this model in response to temperature shift or DNA damage. We conclude that minimal amounts of WTp53 expression are sufficient to enact the p53-dependent G_1 and G_2 checkpoints in MTp53-expressing cells.

WTp53 Expression in H1299-p53^{A138V} Cells Does Not Sensitize Resistant Cells to DNA Breaks or Intrastrand Cross-links: Evidence for GOF for MTp53

The DNA damage imparted by radiotherapy and chemotherapy can elicit apoptosis, mitotic catastrophe, and permanent growth arrest (e.g., tumor cell senescence) in solid tumor cells (2). Radiation and cDDP are used in combination along with other chemotherapies in the treatment of lung cancer. The relative effect of WTp53 over MTp53 on DNA repair and the response to apoptosis or growth arrest may be an important predictor for cell and therapy response and we therefore examined whether WTp53 expression increases cell death in MTp53-expressing H1299 cells.

We first determined the baseline mode of cell death following DNA damage in H1299-p53^{A138V}-expressing cells. To understand the differences in the cellular response to DNA damage in HcRed and HcRed-p53^{A138V} H1299 lung cancer cells, we determined the percentage of cells with γ-H2AX as a function of time following DNA damage at 37°C such that alterations in S phase and G_2 would not occur as this can bias the scoring of γ-H2AX (Fig. 4A). γ-H2AX foci are a useful biomarker for initial and residual DNA DSBs to monitor DNA repair capacity (58, 59). Before irradiation, cells expressing HcRed had twice as many cells containing >5 γ-H2AX foci than cells expressing

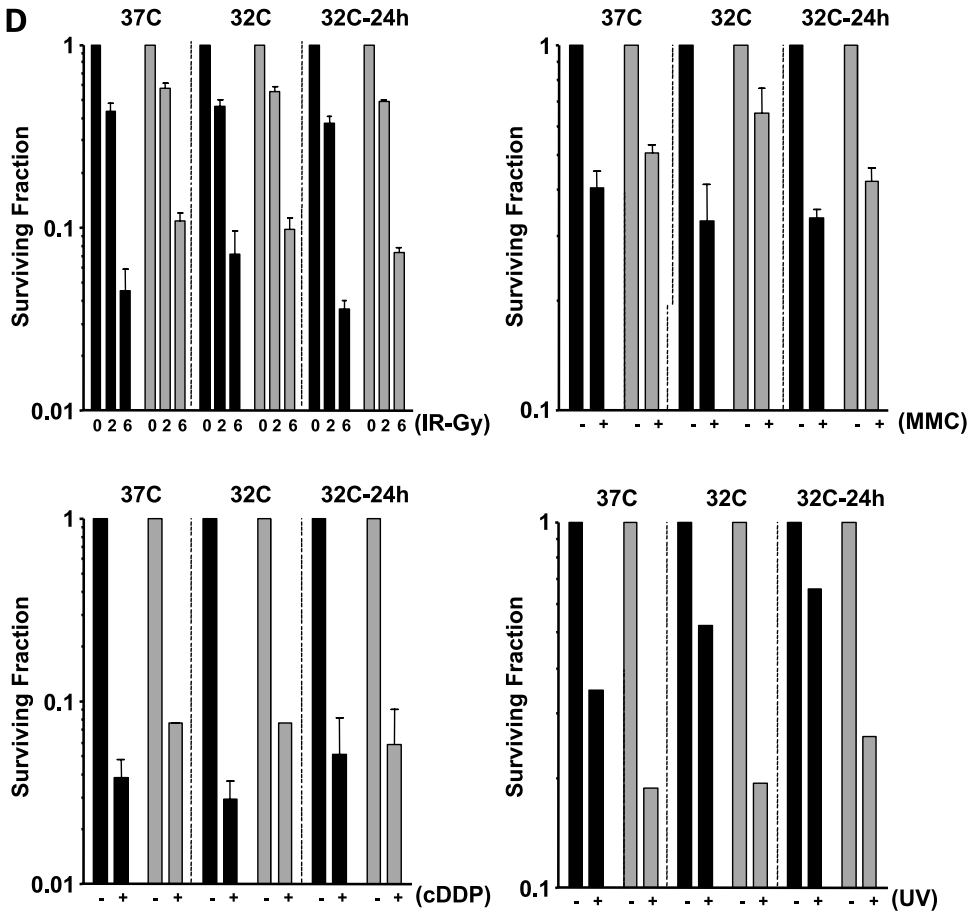

Figure 4 *Continued*. **D,** H1299 cells expressing HcRed (*black columns*) or HcRed-p53^{A138V} (*gray columns*) were exposed to 2 or 6 Gy IR (*top left*), 250 mmol/L MMC (*top right*), 1 μg/μL cDDP (*bottom right*), or 10 J/m^2 UV (*bottom left*). Cells were either maintained at 37°C (*left*), shifted to 32°C for 9 h and immediately back to 37°C following induction of initial DNA damage (*middle*), or maintained at 32°C for a further 24 h during DNA repair before shift to 37°C (*far left*). After 10 days, colonies were stained and counted. *Bars,* SE of three independent experiments. HcRed-p53^{A138V} cells were significantly more resistant than HcRed cells to IR, MMC, and cDDP when treated at 37°C (MTp53) or 32°C (MTp53 + WTp53; $P < 0.05$, paired *t* test); these same cells were significantly more sensitive to UV irradiation under all treatments.

HcRed-p53^{A138V}. Immediately following irradiation, 100% of cells in both populations were γ-H2AX positive, but at 24 and 96 h HcRed cells had a relative greater number of cells with > 5 foci than HcRed-p53^{A138V} cells.

Over the same period, cells were stained for activated caspase-3 as an intracellular marker of apoptosis (60) and counterstained with 4′,6-diamidino-2-phenylindole to examine apoptotic DNA morphology (Fig. 4B). Consistent with all other experiments using this model, the level of apoptosis in both cell lines was very low: <7% following 10 Gy irradiation in both populations. This indicates that although HcRed cells have an increased population of cells with γ-H2AX, this does not reflect an increase in relative radiation-induced apoptosis when compared with HcRed-p53^{A138V} cells. Finally, we stained for the presence of SA-β-galactosidase, which is a marker of increased senescence (61). Nonirradiated cells did not show significant amounts of SA-β-galactosidase (Fig. 4D), whereas SA-β-galactosidase increased qualitatively at 24 and 96 h following DNA damage consistent with terminal arrest and tumor cell senescence as one mode of cell death. Unfortunately, we were unable to quantify the numbers of senescent cells in this assay to determine whether this endpoint correlated to MTp53 expression; however, our data support terminal arrest as an important response in these cell populations.

Novel cancer therapies that can reinstitute WTp53 function through gene expression or pharmacologic means in MTp53-expressing cells have been reported. The efficacy of these treatments will depend on the relative dominance of WTp53 and MTp53 in determining the cell survival of tumor clonogens. We therefore tested the effect of MTp53 alone, or in combination with WTp53, in quantitative long-term colony formation assays. We specifically tested the clonogenic cell sensitivity of HcRed and HcRed-p53^{A138V} cells at 37°C and 32°C to agents that cause DNA damage requiring nonhomologous recombination of DNA DSBs (IR), intrastrand cross-link repair involving homologous recombination (MMC and cDDP), and nucleotide excision repair (UV irradiation). Cells were exposed to varying amounts of IR (2 and 6 Gy; Fig. 4A, *top left*), which causes DSBs, a single dose of cDDP (1 μg/μL; Fig. 4A, *bottom left*), or MMC (250 mmol/L; Fig. 4A, *top right*), both of which cause intrastrand cross-links. Cells were either kept at 37°C throughout the experiment or shifted down to 32°C for 9 h before induction of DNA damage. Following DNA damage, some of these cells were returned to 37°C and the remaining cells were kept at 32°C for an additional 24 h,

during a period of DNA repair, before shifting back to 37°C. Consistent with the cell proliferation data in Fig. 2, maintaining cells at 32°C did not result in any colonies and did not result in usable data.

HcRed cells (Fig. 4A, *black columns*) exhibited a greater degree of sensitivity than cells expressing HcRed-p53^{A138V} (Fig. 4A, *gray columns*) regardless of incubation conditions. Although the increased levels of WTp53 in HcRed-p53^{A138V}-expressing cells kept at 32°C for 24 h may account for the slight decrease in resistance, the fact that it does not match or exceed the sensitivity of HcRed cells suggests a GOF phenotype for the p53^{A138V}. HcRed-p53^{A138V} cells were significantly more resistant than HcRed cells to IR, MMC, and cDDP when treated at 37°C (MTp53) or 32°C (MTp53 + WTp53; $P < 0.05$, paired t test). Importantly, this resistant phenotype is not offset by the expression of functional WTp53 protein. Interestingly, in response to UV radiation (UV, 10 J/m^2; *bottom right*), HcRed-p53^{A138V} cells were much more sensitive to UV radiation compared with cells expressing HcRed only, supporting a strong need for WTp53 in the nucleotide excision repair of UV damage (27).

Discussion

Given the high frequency of p53 mutations in human cancers (62) and the potential effect of p53 status on the response to chemotherapy and radiation therapy (36, 63, 64), studies pertaining to GOF versus dominant-negative behavior of MTp53 proteins are needed to fully understand the role that these mutants have on both tumor progression and resistance to therapy. This is the first study to directly test the effect of MTp53 with or without isogenic short-term WTp53 expression on the response of tumor cells to DNA DSBs and intrastrand and interstrand cross-links. Key findings from the current study include (*a*) human MTp53 can increase resistance by a GOF mechanism to IR, cDDP, and MMC in human lung cancer cells; (*b*) WTp53 is functional when coexpressed with MTp53 leading to p21^{WAF} induction and a G_1 and G_2 checkpoint; (*c*) despite the latter activity, WTp53 cannot override existing MTp53-GOF resistance, suggesting the latter is transcription independent; (*d*) WTp53 expression does not uniformly lead to increased apoptosis when expressed in MTp53-expressing cells; and (*e*) WTp53 is preferentially phosphorylated on Ser^{15} and other residues in comparison with MTp53.

One observation that was consistently made was that p53 localized to the nucleus regardless of the incubation temperature, suggesting that the mutant conformation adopted by the p53^{A138V} mutant is not sufficient to result in cytoplasmic sequestration as has been suggested previously (44, 51, 54). One possibility is that the mutant conformation of the murine p53^{A135V} protein affects the nuclear localization sequence, preventing nuclear localization, whereas the mutant conformation of human p53A138V does not. Alternatively, because cytoplasmic sequestration, which is an active process involving binding to various cytoplasmic proteins, such as HSP70 (53) or vimentin (65), it is also possible that the HcRed tag used in our studies altered the conformation or inhibited the binding to these proteins just enough to make it less amenable to sequestration. However, we observed the same result using a YFP-tagged version of p53^{A138V} (data not shown), suggesting that it is unlikely a specific finding unique to HcRed.

A previous study using the murine p53^{A135V} mutant suggested that the lack of DNA damage–induced NH_2-terminal phosphorylation of the temperature-sensitive p53 at 37°C was due to cytoplasmic sequestration of p53 (54). As stated above, our study showed human p53 was largely localized to the nucleus regardless of conformation; because it was the WTp53 form that became highly phosphorylated following DNA damage (Fig. 3C), this suggests that it is the conformation of p53 that plays a role in the maximal induction of Ser^{15}-p53 phosphorylation. What other modifications p53 might require to maximize its DNA damage response capacity is not known. Immunoprecipitating lysates from HcRed-p53^{A138V} cells that had been irradiated at either 37°C or 32°C with a panel of phosphospecific antibodies following DNA damage showed that no other phosphospecific sites aside from Ser^{15} are significantly up-regulated (data not shown). This is important given the fact that other data from our laboratory showed that transient expression of a codon 15 serine-to-alanine mutant abolished the ability of WTp53 to form DNA damage–induced foci (28). This hints at an important role for p53 phosphorylated at Ser^{15} in the DNA damage recognition/repair capacity of p53. The additional recent report that MTp53 proteins alter MRE11 binding to damaged chromatin suggests transcription-independent role for MTp53 functions in the genetic instability and aggressive tumor cell phenotypes acquired by cells expressing mutant forms of p53 (29, 64, 66).

Similar to p53 transactivation, the heterogenous population of WTp53 and MTp53 in our system did not appear to influence the ability of WTp53 to enact p21^{WAF1} and cell cycle arrests in response to DNA damage (Fig. 3C). Furthermore, the minute amount of WTp53 present in the H1299-p53^{A138V} cells at 37°C (where the vast majority of protein is in the mutant conformation) appeared to have an extremely potent effect of cell cycle arrest without induction of p21^{WAF1}. The ability of WTp53 to induce G_1 arrest without the concomitant induction of p21^{WAF1} has been reported using the temperature-sensitive mutant and may be dependent on cell type or model system (67).

At no point did we see any evidence of apoptosis in this system, suggesting that perhaps H1299 cells are not easily predisposed to p53-induced apoptosis, which is a consistent observation in solid epithelial tumor cell lines (48) and also consistent with previous studies using the murine orthologue (44). Although this article was being written, another report using the p53^{A138V} mutant in human pancreatic cancer cell lines also showed not only a lack of apoptosis but also a lack of induction of Bax (68). However, we cannot rule out the fact that the ongoing presence of MTp53 in the system is playing some

inhibitory role in the apoptotic process either by suppressing proapoptotic pathways or through increased DNA repair. It is noteworthy that Kokontis et al. (69) found that the transactivation function of p53 is both dispensable and inhibitory toward p53-mediated apoptosis. Other cell types may be more susceptible to WTp53-mediated apoptosis as recently reported in TK lymphoblasts isogenic for p53 (70).

Despite the fact that the MTp53 present in the cells did not have a significant effect on WTp53-mediated transactivation and cell cycle control, cells expressing HcRed-p53^{A138V} cells were more resistant to the effects of IR, cDDP, and MMC than HcRed alone cells at 37°C or 32°C. This suggests that either a WTp53 transcription-independent DNA repair pathway or a nonapoptotic cell death pathway(s) may be augmented by MTp53. This is not without precedent (37, 64, 66) and is supported indirectly by the fact that cells expressing HcRed-p53^{A138V} had far fewer γ-H2AX foci following DNA damage regardless of the temperature they were maintained at following DNA damage. Although the reported ability of MTp53 to upregulate the multidrug resistance protein MRP1 (71, 72) might explain the resistance of HcRed-p53^{A138V} cells to cDDP and MMC, it would not account for the resistance to IR-induced DNA damage. Exposure to UV radiation had the opposite effect: HcRed-p53^{A138V} cells were much more sensitive to UV-induced DNA damage. Given the well-characterized role for WTp53 in nucleotide excision repair (73), the presence of MTp53 in this case is perhaps having a dominant-negative effect on the ability of WTp53 to perform its nucleotide excision repair function properly and thus negatively affects cell survival following UV damage.

In summary, the H1299-p53^{A138V} cells are a robust model system to study coexpression of WTp53 and MTp53 for a variety of experimental endpoints. However, this only represents one particular temperature-sensitive mutant; other mutants of p53 have been described with temperature sensitivity (74–76). Further experiments using other temperature-sensitive mutants may allow a greater understanding of the effect of different core domain p53 mutants in altering tumor cell survival to cancer therapies. When taken together, these results suggest that a therapeutic maneuver that solely reintroduces WTp53 expression (e.g., adenoviral WTp53 therapies) on a MTp53 background may not necessarily overcome MTp53-mediated resistance. This could explain suboptimal responses in some patients using adenoviral WTp53 therapy in clinical trials (31, 33). Clinical trials are awaited for compounds, such as PRIMA-1 (34), which can revert MTp53 back into a WTp53 conformation (as monotherapy or an adjunct to radiotherapy and chemotherapy) to determine their relative efficacy as p53-targeting agents. The development of rapid assays that can clinically test for dominant-negative versus GOF activity for p53 mutants in tumor biopsies derived form patients may allow for better prediction of therapy response and triaging of best therapies for a given individual patient.

Acknowledgments

We thank the Bristow laboratory for encouragement and critical comments and A. Choudhury for technical expertise.

References

1. Willers H, Dahm-Daphi J, Powell SN. Repair of radiation damage to DNA. Br J Cancer 2004;90:1297 – 301.

2. Faulhaber O, Bristow RG. Basis of cell kill following clinical radiotherapy. In: Sluyser M, editor. Application of apoptosis to cancer treatment. The Netherlands: Springer; 2005. p. 293 – 320.

3. Cuddihy AR, Bristow RG. The p53 protein family and radiation sensitivity: yes or no? Cancer Metastasis Rev 2004;23:237 – 57.

4. Petitjean A, Achatz MI, Borresen-Dale AL, Hainaut P, Olivier M. TP53 mutations in human cancers: functional selection and impact on cancer prognosis and outcomes. Oncogene 2007;26:2157 – 65.

5. Levine AJ. p53, the cellular gatekeeper for growth and division. Cell 1997;88:323 – 31.

6. Harris SL, Levine AJ. The p53 pathway: positive and negative feedback loops. Oncogene 2005;24:2899 – 908.

7. Ashcroft M, Vousden KH. Regulation of p53 stability. Oncogene 1999; 18:7637 – 43.

8. Kubbutat MH, Ludwig RL, Ashcroft M, Vousden KH. Regulation of Mdm2-directed degradation by the C terminus of p53. Mol Cell Biol 1998; 18:5690 – 8.

9. Haupt Y, Maya R, Kazaz A, Oren M. Mdm2 promotes the rapid degradation of p53. Nature 1997;387:296 – 9.

10. Michael D, Oren M. The p53-2 module and the ubiquitin system. Semin Cancer Biol 2003;13:49 – 58.

11. Appella E, Anderson CW. Post-translational modifications and activation of p53 by genotoxic stresses. Eur J Biochem 2001;268:2764 – 72.

12. Meek DW. The p53 response to DNA damage. DNA Repair (Amst) 2004;3:1049 – 56.

13. Dauth I, Kruger J, Hofmann TG. Homeodomain-interacting protein kinase 2 is the ionizing radiation-activated p53 serine 46 kinase and is regulated by ATM. Cancer Res 2007;67:2274 – 9.

14. El-Deiry W, Tokino T, Velculescu VE, et al. WAF1, a potential mediator of p53 tumor suppression. Cell 1993;75:817 – 25.

15. Harper JW, Adami GR, Wei N, Keyomarsi K, Elledge SJ. The p21 cdk-inhibitor protein cip1 is a potent inhibitor of G_1 cyclin-dependent kinases. Cell 1993;75:805 – 16.

16. Hermeking H, Lengauer C, Polyak K, et al. 14-3-3σ is a p53-regulated inhibitor of G_2-M progression. Mol Cell 1997;1:3 – 11.

17. Doumont G, Martoriati A, Beekman C, et al. G_1 checkpoint failure and increased tumor susceptibility in mice lacking the novel p53 target Ptprv. EMBO J 2005;24:3093 – 103.

18. Miyashita T, Reed JC. Tumor suppressor p53 is a direct transcriptional activator of the human bax gene. Cell 1995;80:293 – 9.

19. Nakano K, Vousden KH. PUMA, a novel proapoptotic gene, is induced by p53. Mol Cell 2001;7:683 – 94.

20. Oda E, Ohki R, Murasawa H, et al. Noxa, a BH3-only member of the Bcl-2 family and candidate mediator of p53-induced apoptosis. Science 2000;288:1053 – 8.

21. Polyak K, Xia Y, Zweier JL, Kinzler KW, Vogelstein B. A model for p53-induced apoptosis. Nature 1997;389:300 – 5.

22. Benchimol S. p53-dependent pathways of apoptosis. Cell Death Differ 2001;8:1049 – 51.

23. Moll UM, Wolff S, Speidel D, Deppert W. Transcription-independent pro-apoptotic functions of p53. Curr Opin Cell Biol 2005;17:631 – 6.

24. Wiesmuller L. Genetic stabilization by p53 involves growth regulatory and repair pathways. J Biomed Biotechnol 2001;1:7 – 10.

25. Albrechtsen N, Dornreiter I, Grosse F, Kim E, Wiesmuller L, Deppert W. Maintenance of genomic integrity by p53: complementary roles for activated and non-activated p53. Oncogene 1999;18:7706 – 17.

26. Adimoolam S, Lin CX, Ford JM. The p53-regulated cyclin-dependent kinase inhibitor, p21 (cip1, waf1, sdi1), is not required for global genomic and transcription-coupled nucleotide excision repair of UV-induced DNA photoproducts. J Biol Chem 2001;276:25813 – 22.

27. Cistulli CA, Kaufmann WK. p53-dependent signaling sustains DNA

replication and enhances clonogenic survival in 254 nm ultraviolet-irradiated human fibroblasts. Cancer Res 1998;58:1993 – 2002.

28. Al Rashid ST, Dellaire G, Cuddihy A, et al. Evidence for the direct binding of phosphorylated p53 to sites of DNA breaks *in vivo*. Cancer Res 2005;65:10810 – 21.

29. Song H, Hollstein M, Xu Y. p53 gain-of-function cancer mutants induce genetic instability by inactivating ATM. Nat Cell Biol 2007;9:573 – 80.

30. Bristow RG, Hu Q, Jang A, et al. Radioresistant MTp53-expressing rat embryo cell transformants exhibit increased DNA-dsb rejoining during exposure to ionizing radiation. Oncogene 1998;16:1789 – 802.

31. Huang CL, Yokomise H, Miyatake A. Clinical significance of the p53 pathway and associated gene therapy in non-small cell lung cancers. Future Oncol 2007;3:83 – 93.

32. Vikhanskaya F, Lee MK, Mazzoletti M, Broggini M, Sabapathy K. Cancer-derived p53 mutants suppress p53-target gene expression-potential mechanism for gain of function of mutant p53. Nucleic Acids Res 2007;35:2093 – 104.

33. Fujiwara T, Tanaka N, Kanazawa S, et al. Multicenter phase I study of repeated intratumoral delivery of adenoviral p53 in patients with advanced non-small-cell lung cancer. J Clin Oncol 2006;24:1689 – 99.

34. Wiman KG. Restoration of wild-type p53 function in human tumors: strategies for efficient cancer therapy. Adv Cancer Res 2007;97:321 – 38.

35. Strano S, Dell'Orso S, Di Agostino S, Fontemaggi G, Sacchi A, Blandino G. Mutant p53: an oncogenic transcription factor. Oncogene 2007;26:2212 – 9.

36. Blandino G, Levine AJ, Oren M. Mutant p53 gain of function: differential effects of different p53 mutants on resistance of cultured cells to chemotherapy. Oncogene 1999;18:477 – 85.

37. Bristow RG, Peacock J, Jang A, Kim J, Hill RP, Benchimol S. Resistance to DNA-damaging agents is discordant from experimental metastatic capacity in MEF ras-transformants-expressing gain of function MTp53. Oncogene 2003;22:2960 – 6.

38. Wong RP, Tsang WP, Chau PY, Co NN, Tsang TY, Kwok TT. p53 – 273H gains new function in induction of drug resistance through down-regulation of procaspase-3. Mol Cancer Ther 2007;6:1054 – 61.

39. Tsang WP, Ho FY, Fung KP, Kong SK, Kwok TT. p53-175H mutant gains new function in regulation of doxorubicin-induced apoptosis. Int J Cancer 2005;114:331 – 6.

40. Kaeser MD, Pebernard S, Iggo RD. Regulation of p53 stability and function in HCT116 colon cancer cells. J Biol Chem 2004;279:7598 – 605.

41. Mazzatti DJ, Lee YJ, Helt CE, O'Reilly MA, Keng PC. p53 modulates radiation sensitivity independent of p21 transcriptional activation. Am J Clin Oncol 2005;28:43 – 50.

42. Diller L, Kassel J, Nelson CE, et al. p53 functions as a cell cycle control protein in osteosarcomas. Mol Cell Biol 1990;10:5772 – 81.

43. Michalovitz D, Halevy O, Oren M. Conditional inhibition of transformation and of cell proliferation by a temperature-sensitive mutant of p53. Cell 1990;62:671 – 80.

44. Martinez J, Georgoff I, Martinez J, Levine AJ. Cellular localization and cell cycle regulation by a temperature-sensitive p53 protein. Genes Dev 1991;5:151 – 9.

45. Koniaras K, Cuddihy AR, Christopoulos H, Hogg A, O'Connell MJ. Inhibition of Chk1-dependent G_2 DNA damage checkpoint radiosensitizes p53 mutant human cells. Oncogene 2001;20:7453 – 63.

46. Dignam JD, Martin PL, Shastry BS, Roeder RG. Eukaryotic gene transcription with purified components. Methods Enzymol 1983;101:582 – 98.

47. Wong ML, Medrano JF. Real-time PCR for mRNA quantitation. Biotechniques 2005;39:75 – 85.

48. Bromfield GP, Meng A, Warde P, Bristow RG. Cell death in irradiated prostate epithelial cells: role of apoptotic and clonogenic cell kill. Prostate Cancer Prostatic Dis 2003;6:73 – 85.

49. Yamato K, Yamamoto M, Hirano Y, Tsuchida N. A human temperature-sensitive p53 mutant p53Val-138: modulation of the cell cycle, viability and expression of p53-responsive genes. Oncogene 1995;11:1 – 6.

50. Deppert W, Gohler T, Koga H, Kim E. Mutant p53: ''gain of function'' through perturbation of nuclear structure and function? J Cell Biochem Suppl 2000;Suppl 35:115 – 22.

51. Ginsberg D, Michael-Michalovitz D, Oren M. Induction of growth arrest by a temperature-sensitive p53 mutant is correlated with increased nuclear localization and decreased stability of the protein. Mol Cell Biol 1991;11:582 – 5.

52. Milner J, Medcalf EA. Cotranslation of activated mutant p53 with wild type drives the wild-type p53 protein into the mutant conformation. Cell 1991;65:765 – 74.

53. Gannon JV, Greaves R, Iggo R, Lane DP. Activating mutations in p53 produce a common conformational effect. A monoclonal antibody specific for the mutant form. EMBO J 1990;9:1595 – 602.

54. Martinez JD, Craven MT, Joseloff E, Milczarek G, Bowden GT. Regulation of DNA binding and transactivation in p53 by nuclear localization and phosphorylation. Oncogene 1997;14:2511 – 20.

55. Ullrich SJ, Sakaguchi K, Lees-Miller SP, et al. Phosphorylation at Ser-15 and Ser-392 in mutant p53 molecules from human tumors is altered compared to wild-type p53. Proc Natl Acad Sci U S A 1993;90:5954 – 8.

56. Jackson MW, Agarwal MK, Agarwal ML, et al. Limited role of N-terminal phosphoserine residues in the activation of transcription by p53. Oncogene 2004;23:4477 – 87.

57. Prigent C, Dimitrov S. Phosphorylation of serine 10 in histone H3, what for? J Cell Sci 2003;116:3677 – 85.

58. Fernandez-Capetillo O, Lee A, Nussenzweig M, Nussenzweig A. H2AX: the histone guardian of the genome. DNA Repair (Amst) 2004;3: 959 – 67.

59. Lowndes NF, Toh GW. DNA repair: the importance of phosphorylating histone H2AX. Curr Biol 2005;15:R99 – 102.

60. Riedl SJ, Shi Y. Molecular mechanisms of caspase regulation during apoptosis. Nat Rev Mol Cell Biol 2004;5:897 – 907.

61. Dimri GP, Lee X, Basile G, et al. A biomarker that identifies senescent human cells in culture and in aging skin *in vivo*. Proc Natl Acad Sci U S A 1995;92:9363 – 7.

62. Hainaut P, Hernandez T, Robinson A, et al. IARC Database of p53 gene mutations in human tumors and cell lines: updated compilation, revised formats and new visualisation tools. Nucleic Acids Res 1998;26: 205 – 13.

63. Bristow RG, Brail L, Jang A, et al. P53-mediated radioresistance does not correlate with metastatic potential in tumorigenic rat embryo cell lines following oncogene transfection. Int J Radiat Oncol Biol Phys 1996;34: 341 – 55.

64. Sigal A, Rotter V. Oncogenic mutations of the p53 tumor suppressor: the demons of the guardian of the genome. Cancer Res 2000;60:6788 – 93.

65. Klotzsche O, Etzrodt D, Hohenberg H, Bohn W, Deppert W. Cytoplasmic retention of mutant tsp53 is dependent on an intermediate filament protein (vimentin) scaffold. Oncogene 1998;16:3423 – 34.

66. Kim E, Deppert W. Transcriptional activities of mutant p53: when mutations are more than a loss. J Cell Biochem 2004;93:878 – 86.

67. Hirano Y, Yamato K, Tsuchida N. A temperature sensitive mutant of the human p53, Val138, arrests rat cell growth without induced expression of cip1/waf1/sdi1 after temperature shift-down. Oncogene 1995;10:1879 – 85.

68. Nuevemann D, Christgen M, Ungefroren H, Kalthoff H. Stable expression of temperature-sensitive p53: a suitable model to study wild-type p53 function in pancreatic carcinoma cells. Oncol Rep 2006;16:575 – 9.

69. Kokontis JM, Wagner AJ, O'Leary M, Liao S, Hay N. A transcriptional activation function of p53 is dispensable for and inhibitory of its apoptotic function. Oncogene 2001;20:659 – 68.

70. Zhang Q, Liu Y, Zhou J, Chen W, Zhang Y, Liber HL. Wild-type p53 reduces radiation hypermutability in p53-mutated human lymphoblast cells. Mutagenesis 2007;22:329 – 34.

71. Tsang WP, Chau SP, Fung KP, Kong SK, Kwok TT. Modulation of multidrug resistance-associated protein 1 (MRP1) by p53 mutant in Saos-2 cells. Cancer Chemother Pharmacol 2003;51:161 – 6.

72. Sullivan GF, Yang JM, Vassil A, Yang J, Bash-Babula J, Hait WN. Regulation of expression of the multidrug resistance protein MRP1 by p53 in human prostate cancer cells. J Clin Invest 2000;105:1261 – 7.

73. Smith ML, Seo YR. p53 regulation of DNA excision repair pathways. Mutagenesis 2002;17:149 – 56.

74. Buckbinder L, Talbott R, Seizinger BR, Kley N. Gene regulation by temperature-sensitive p53 mutants: identification of p53 response genes. Proc Natl Acad Sci U S A 1994;91:10640 – 4.

75. Medcalf EA, Takahashi T, Chiba I, Minna J, Milner J. Temperature-sensitive mutants of p53 associated with human carcinoma of the lung. Oncogene 1992;7:71 – 6.

76. Zhang W, Guo XY, Hu GY, Liu WB, Shay JW, Deisseroth AB. A temperature-sensitive mutant of human p53. EMBO J 1994;13:2535 – 44.